

OLALa: Online Learned Adaptive Lattice Codes for Heterogeneous Federated Learning

Natalie Lang*, Maya Simhi*, and Nir Shlezinger

Abstract—Federated learning (FL) enables collaborative training across distributed clients without sharing raw data, often at the cost of substantial communication overhead induced by transmitting high-dimensional model updates. This overhead can be alleviated by having the clients quantize their model updates, with dithered lattice quantizers identified as an attractive scheme due to its structural simplicity and convergence-preserving properties. However, existing lattice-based FL schemes typically rely on a fixed quantization rule, which is suboptimal in heterogeneous and dynamic environments where the model updates distribution varies across users and training rounds. In this work, we propose *Online Learned Adaptive Lattices (OLALa)*, a heterogeneous FL framework where each client can adjust its quantizer online using lightweight local computations. We first derive convergence guarantees for FL with non-fixed lattice quantizers and show that proper lattice adaptation can tighten the convergence bound. Then, we design an online learning algorithm that enables clients to tune their quantizers throughout the FL process while exchanging only a compact set of quantization parameters. Numerical experiments demonstrate that OLALa consistently improves learning performance under various quantization rates, outperforming conventional fixed-codebook and non-adaptive schemes.

I. INTRODUCTION

THE machine learning framework of federated learning (FL) has multiple clients collaboratively train a global model under the orchestration of a central server, while keeping their local data private [2]. By transmitting only model updates rather than raw data, FL enables the utilization of distributed datasets without requiring private data to be shared [3]–[5].

One of the principal challenges of FL, that is largely absent in centralized learning setups, is the substantial communication overhead stemming from the frequent exchange of high-dimensional model updates between the server and the distributed clients [5]. This communication bottleneck is particularly critical in bandwidth-limited or wireless environments, where the transmission cost can dominate the training process [6]. As a result, a broad range of techniques have been proposed to mitigate communication load, including client selection strategies [7], [8], update sparsification [9]–[11], and over-the-air aggregation schemes [12]–[14]. A prominent and widely adopted approach is *model compression*, wherein each client transmits a compressed representation of its local update [15]. In particular, lossy compression methods, and notably quantization [16]–[20], have demonstrated significant effectiveness in reducing communication costs while maintaining acceptable learning performance [21].

Generally speaking, quantization can be represented as a codebook of digital representations [22]. Such codebooks can be tuned from data using classic clustering-type methods [23], [24], with more recent techniques employing deep learning [25], [26]. In practice, one is often interested in utilizing structured mappings, and particularly uniform quantizers and their vector general form of *lattice quantizers*, as opposed to arbitrary codebooks [27]. Such structured quantizers are simple, support nested implementations [28], and, when combined with dithering [29], [30], can eliminate dependence between the distortion and the signal [31]. Such forms of dithered quantization are considered to be highly suitable for model update compression in FL, due their ability to preserve convergence of the training procedure [16], [19], while potentially enhancing privacy preservation [32]–[34].

The mapping of a lattice quantizer is determined by its *generator matrix* and the associated distance metric [35]. Traditional designs of dithered lattice quantizers leverage their tractable rate-distortion behavior under the assumption that the quantizer is not overloaded. This property allows for analytical bounds on the quantization error characterized in terms of the lattice second-order moment to guide the design [36], either through closed-form expressions in special cases [37], [38] or by iterative optimization procedures [39], [40]. Alternatively, our preliminary study [1] showed that deep learning tools can learn lattice quantizers that directly minimize distortion without relying on non-overload analytical bounds, by converting the quantizer into a trainable discriminative model [41]. In the context of FL, these strategies result in a single, fixed quantization rule that is uniformly applied across all clients and throughout all communication rounds. However, due to the inherent statistical (data distribution) heterogeneity of FL [42], combined with the evolving nature of model updates over time, the distribution of the weights to be quantized can vary significantly across clients and iterations. Moreover, these variations are often difficult to predict or model in advance, indicating that a one-size-fits-all lattice design may be suboptimal for FL.

In this work, we study heterogeneous FL under user- and time-varying adaptive quantization, motivated by the need to support dynamic and non-stationary weight distributions across clients and communication rounds. We introduce *Online Learned Adaptive Lattices (OLALa)*, a framework that enables locally adaptive dithered lattice quantization tailored to the evolving characteristics of each client's updates. A key insight underlying OLALa is that dithered lattice quantizers are particularly well-suited to this setting, as their overall behavior is governed by the compact generator matrix, whose dimensionality is independent of the quantization rate. This structural property makes them ideal for online adaptation: clients can efficiently adjust their quantizers

*Equal contribution. The preliminary findings of this work were presented in the 2024 IEEE International Conference on Acoustics, Speech, and Signal Processing (ICASSP) as the paper [1]. The authors are with the School of ECE, Ben-Gurion University of the Negev Be'er-Sheva, Israel. Emails: {langn, mayasimh}@post.bgu.ac.il, nirshl@bgu.ac.il

on-the-fly based on local statistics and communicate the updated parameters to the server with negligible communication overhead, thus not being restricted to pre-determined compression rule as in alternative forms of learned local mappings [15].

To motivate the design of OLALa, we begin by providing a theoretical analysis of the convergence behavior of heterogeneous FL when employing non-identical, adaptive lattice quantizers. Under standard assumptions on the learning model and data distribution [43], we rigorously prove that the training process converges to the minimizer of the empirical risk, and that when operating with a fixed compression bit budget, the convergence bound can be tightened through appropriate adaptive lattice design.

Building on this insight, we develop an online learning algorithm based on model-based deep learning principles [44], which enables each client to dynamically adapt its lattice quantizer throughout the FL process. Our approach draws insights from [45], utilizing dedicated fixed-input deep neural network (DNN) during training to learn how to represent the generator matrix, combined with a novel casting of the quantizer mapping that enables gradient-based learning. The resulting OLALa learns user- and time-specific lattices using lightweight local computations and communicates only a compact set of quantizer metadata, thereby maintaining a low communication footprint. Our experiments demonstrate that OLALa effectively reduces the quantization distortion, i.e., improving its associated mean squared error (MSE), and yields superior learning performance across a wide range of quantization rates.

The rest of this paper is organized as follows: Section II reviews preliminaries in FL and lattice quantization. Section III introduces the OLALa framework, motivates using adaptive lattices via a theoretical convergence analysis, and details the proposed online learning scheme. We numerically evaluate OLALa in Section IV, with concluding remarks provided in Section V.

Throughout this paper, we use boldface lower-case letters for vectors, e.g., \mathbf{x} . We use calligraphic letters for sets, e.g., \mathcal{X} , with $|\mathcal{X}|$ being its cardinality. The stochastic expectation, variance, inner product, and ℓ_2 norm are denoted by $\mathbb{E}[\cdot]$, $\text{Var}(\cdot)$, $\langle \cdot; \cdot \rangle$, and $\|\cdot\|$, respectively; while \mathbb{R} is the set of real numbers.

II. SYSTEM MODEL AND PRELIMINARIES

In this section, we set the ground for the derivation of OLALa. We commence by presenting the system model of FL in Subsection II-A. Then, we provide a description of lattice-based compression in Subsection II-B.

A. Federated Learning

The FL paradigm [2] constitutes a central server training a parameterized model $\mathbf{w} \in \mathbb{R}^m$, utilizing data stored at a group of U users indexed by $u \in \{1, \dots, U\}$. Unlike traditional centralized learning, their corresponding datasets, denoted $\mathcal{D}_1, \mathcal{D}_2, \dots, \mathcal{D}_U$, cannot be transferred to the server due to privacy or communication restrictions. Letting $F_u(\mathbf{w})$ denote the empirical risk function of the u th user, FL aims to find the model parameters that minimize the averaged empirical risk across all users, i.e.,

$$\mathbf{w}_{\text{opt}} = \arg \min_{\mathbf{w}} \left\{ F(\mathbf{w}) \triangleq \frac{1}{U} \sum_{u=1}^U F_u(\mathbf{w}) \right\}. \quad (1)$$

In (1), it is assumed (for simplicity) that the local datasets are of the same cardinality, and that all devices participate in training.

FL follows an iterative procedure operated in rounds [5]. In the t th round, the server transmits the current global model \mathbf{w}_t to the clients, who each updates the model using its local dataset and computational resources. These updates are then sent back to the server, which aggregates them to form the new global model. FL typically involves training at the devices via variants of local-stochastic gradient descent (SGD) [46], which, in its simplest form, updates the weights via

$$\mathbf{w}_{t+1}^u \leftarrow \mathbf{w}_t - \eta_t \nabla F_u(\mathbf{w}_t; i_t^u); \quad (2)$$

where i_t^u is the data sample index chosen uniformly from \mathcal{D}_u , and η_t is the learning rate. In general, the client can replace (2) with multiple local iterations, and convey the model update $\mathbf{h}_t^u := \mathbf{w}_{t+1}^u - \mathbf{w}_t$. The model updates are aggregated by the server, most commonly using federated averaging (FedAvg) [2], i.e.,

$$\mathbf{w}_{t+1} \triangleq \frac{1}{U} \sum_{u=1}^U \mathbf{w}_{t+1}^u = \mathbf{w}_t + \frac{1}{U} \sum_{u=1}^U \mathbf{h}_t^u. \quad (3)$$

The above conventional FL formulation gives rise to several key challenges, that are not present in centralized learning [6]. For once, the distribution of the datasets often varies between the users. This form of *statistical heterogeneity* indicates that the distribution of the local updates \mathbf{h}_t^u can vary considerably between different users [42]. Moreover, broadcasting the local update of each single edge client results in a frequent exchange of high-dimensional parameter vectors to enable aggregation via (3). This *communication overhead* can possibly load the communication network. The latter is often tackled by integration of quantization techniques, discussed next.

B. Lattice Coding

Quantization refers to the representation of continuous-valued signals via finite-bit representations [22]. The tradeoff between the quantization rate and the distortion induced by the quantization operation can be improved by jointly quantizing multiple samples via *vector quantization* [47]. A leading approach to implement vector quantizers is based on lattice quantization [31]:

Definition II.1 (Lattice Quantizer). A *lattice quantizer* of dimension $L \in \mathbb{Z}^+$ and generator matrix $\mathbf{G} \in \mathbb{R}^{L \times L}$ maps a continuous-valued vector $\mathbf{x} \in \mathbb{R}^L$ into a discrete representation $Q_{\mathcal{L}}(\mathbf{x})$ by selecting the nearest point in the (Voronoi-cells) lattice $\mathcal{L} \triangleq \{\mathbf{G}\mathbf{l} : \mathbf{l} \in \mathbb{Z}^L\}$, i.e.,

$$Q_{\mathcal{L}}(\mathbf{x}) = \arg \min_{\mathbf{z} \in \mathcal{L}} \|\mathbf{x} - \mathbf{z}\|. \quad (4)$$

To apply $Q_{\mathcal{L}}$ to a vector $\mathbf{x} \in \mathbb{R}^{ML}$, it is divided into $[\mathbf{x}_1, \dots, \mathbf{x}_M]^T$, and each sub-vector is quantized separately.

It is noted that for $L = 1$, $Q_{\mathcal{L}}(\cdot)$ in (4) specializes scalar uniform quantization. While quantizing via (4) formally requires exhaustive search, it can be approached using computationally efficient methods [48].

A lattice \mathcal{L} partitions \mathbb{R}^L into cells centered around the lattice points, where the basic cell is

$$\mathcal{P}_0 = \{\mathbf{x} : Q_{\mathcal{L}}(\mathbf{x}) = \mathbf{0}\}. \quad (5)$$

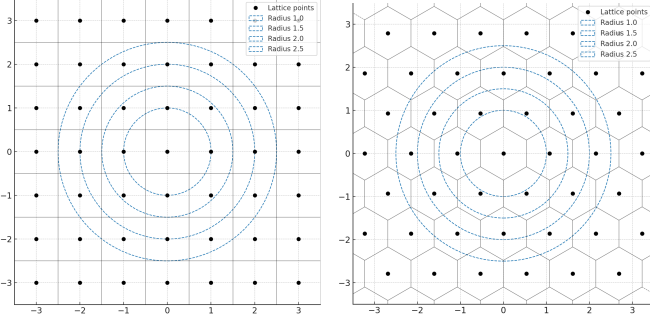


Fig. 1: Example: truncated lattices structures. \bullet 's mark lattice points (codewords); concentric circles represent the radii (i.e., γ values). The left quantizer has the identity as its generator matrix, while the right has the hexagonal generator matrix scaled to have unit determinant.

The number of lattice points in \mathcal{L} is countable but infinite. Thus, to obtain a finite-bit representation, it is common to restrict \mathcal{L} to include only points in a given sphere of radius γ , \mathcal{L}_γ , i.e.,

$$\mathcal{L}_\gamma \triangleq \{z \in \mathcal{L} : \|z\| \leq \gamma\}. \quad (6)$$

The number of lattice points, $|\mathcal{L}_\gamma|$, dictates the number of bits per sample, via the quantization rate $R \triangleq \frac{1}{L} \log_2(|\mathcal{L}_\gamma|)$. An event in which the input to the lattice quantizer does not reside in this sphere is referred to as *overloading*, from which quantizers are typically designed to avoid [22]. Fig. 1 demonstrates different truncated lattices configurations in the 2D plane, i.e., $L = 2$.

Lattice quantization yields a distortion term $e \triangleq Q_{\mathcal{L}}(\mathbf{x}) - \mathbf{x}$ that is deterministically determined by \mathbf{x} . To be made stochastic, it is often combined with *probabilistic quantization*, and particularly with subtractive dithered quantization (SDQ) [29], [30]:

Definition II.2 (SDQ). *Let \mathbf{d} be drawn uniformly from \mathcal{P}_0 in (5). The SDQ of $\mathbf{x} \in \mathbb{R}^L$ with lattice \mathcal{L} is given by*

$$Q_{\mathcal{L}}^{\text{SDQ}}(\mathbf{x}) = Q_{\mathcal{L}}(\mathbf{x} + \mathbf{d}) - \mathbf{d}. \quad (7)$$

A key property of SDQ stems from the fact that its resulting distortion can be made independent of the quantized input, as stated in [29, Thm. 1], recalled below as Theorem II.3:

Theorem II.3. *Consider a quantizer induced by a γ -supported lattice $\mathcal{L}_\gamma(\mathbf{G})$, with input vectors $\{\mathbf{x}_i\}$ and dither vectors $\{\mathbf{d}_i\}$, where each \mathbf{d}_i is uniformly distributed over the basic cell \mathcal{P}_0 defined in (5). Then, if the quantizer is not over-loaded, i.e., $\forall i, \Pr(\|\mathbf{x}_i + \mathbf{d}_i\| < \gamma) = 1$, the SDQ errors, defined as*

$$\begin{aligned} e_i^{\text{SDQ}} &:= Q_{\mathcal{L}_\gamma(\mathbf{G})}^{\text{SDQ}}(\mathbf{x}_i) - \mathbf{x}_i \\ &= \arg \min_{\mathbf{l} \in \mathcal{L}_\gamma(\mathbf{G})} \|\mathbf{x}_i + \mathbf{d}_i - \mathbf{l}\| - \mathbf{d}_i - \mathbf{x}_i \end{aligned} \quad (8)$$

are mutually independent of $\{\mathbf{x}_i\}$; and obey an i.i.d uniform distribution over the basic lattice cell. That is, $\mathbb{E}[e_i^{\text{SDQ}}] = 0$ and

$$\text{Var}(e_i^{\text{SDQ}}) = \mathbb{E}[\|e_i^{\text{SDQ}}\|^2] = \sigma_{\text{SDQ}}^2(\mathcal{L}_\gamma(\mathbf{G})) \quad \forall i, \quad (9)$$

where $\sigma_{\text{SDQ}}^2(\mathcal{L}_\gamma(\mathbf{G}))$ is the MSE per dimension [35],

$$\sigma_{\text{SDQ}}^2(\mathcal{L}_\gamma(\mathbf{G})) := \frac{1}{L} \cdot \frac{\int_{\mathcal{P}_0} \|\mathbf{x}\|^2 d\mathbf{x}}{\text{Vol}(\mathcal{P}_0)}; \quad (10)$$

and $\text{Vol}(\mathcal{P}_0)$ is the volume of \mathcal{P}_0 .

Theorem II.3 indicates that when the quantizer is not overloaded, the distortion induced by SDQ can be modeled as white noise uniformly distributed over \mathcal{P}_0 . It also implies that, for any input vector residing within the support of the truncated-lattice, SDQ with multivariate lattice quantization yields distortion with lesser variance compared to uniform scalar quantizers with the same number of bits per sample [35].

III. ONLINE ADAPTIVE LATTICE LEARNING

In this section we introduce the proposed OLALa framework. We start in Subsection III-A by explaining the operation of FL with lattice quantizers in which the lattices are allowed to vary, without specifying how they are being set. Then, we theoretically analyze the convergence profile of the resulting FL framework in Subsection III-B, indicating the theoretical potential gains of adapting the lattices between users and rounds in heterogeneous settings. This leads us to the presentation of our method for online learning of the lattices in Subsection III-C, which is followed by a discussion in Subsection III-D.

A. FL with Adaptive Lattice Quantizers

We begin by describing a generic FL setup where the users employ adaptive lattice-based compression. In this configuration, each communication round consists of both model updates and lattice quantizer metadata that evolve over time. Accordingly, the global model \mathbf{w}_t in (3), which is the desired FedAvg outcome, and the local updates \mathbf{h}_t^u , are respectively replaced with $\tilde{\mathbf{w}}_t$ and $\tilde{\mathbf{h}}_t^u$. The procedure, detailed in Algorithm 1, operates iteratively: in each round t , the server broadcasts the current global model $\tilde{\mathbf{w}}_{t-1}$ to all participating users; followed by user-side encoding and server-side decoding.

1) *User-Side Encoding:* Each user u locally updates the model to obtain $\tilde{\mathbf{h}}_t^u$ via, e.g., local SGD (2). To reduce the cost of uplink communication, the update is compressed using a dithered lattice quantizer. The lattice chosen by user u at round t , characterized by a generator matrix \mathbf{G}_t^u and support radius γ_t^u , is selected such that the resulting quantizer operates at a fixed target rate R . While here we do not specify how the choice of the lattice (i.e., \mathbf{G}_t^u and γ_t^u in Step 5 of Algorithm 1) is done, we propose an online learning method for that aim in Subsection III-C. The dither signal \mathbf{d}_t^u is independently generated using a shared pseudo-random seed ξ_t^u (which can be set once when initializing the FL procedure), enabling the server to reconstruct the same dither.

Finally, the user transmits to the server the quantized model update $Q_{\mathcal{L}_{\gamma_t^u}(\mathbf{G}_t^u)}(\tilde{\mathbf{h}}_t^u + \mathbf{d}_t^u)$ along with the metadata \mathbf{G}_t^u . Note that, if we assume the metadata is sent with high-resolution, e.g., 64 bits representation, the overall number of bits conveyed is $m \cdot R + 64 \cdot L^2$, which is a minor overhead when training large models (i.e., large m).

2) *Server-Side Decoding:* Upon reception, the server reconstructs the dither vector \mathbf{d}_t^u using ξ_t^u and recovers the compressed model via subtracting the dither, obtaining the SDQ of \mathbf{w}_t^u . The global model is then updated by aggregating these quantized updates across all users, typically via FedAvg, i.e.,

$$\tilde{\mathbf{w}}_t = \tilde{\mathbf{w}}_{t-1} + \frac{1}{U} \sum_{u=1}^U Q_{\mathcal{L}_{\gamma_t^u}(\mathbf{G}_t^u)}^{\text{SDQ}}(\tilde{\mathbf{h}}_t^u). \quad (11)$$

Algorithm 1: FL with Adaptive Lattice Quantizers

Init: Data sets $\{\mathcal{D}_u\}$, lattice dimension L , rate R ;
 Initial model parameters \mathbf{w}_0 , random seeds $\{\xi_t^u\}$

```

1 for  $t = 1, 2 \dots$  do
  Server side:
2   Send global model  $\tilde{\mathbf{w}}_{t-1}$  to all users;
3   for  $u = 1, 2, \dots, U$  do
    User  $u$  side:
4     Obtain  $\tilde{\mathbf{h}}_t^u$  via local training on  $\mathcal{D}_u$  from  $\tilde{\mathbf{w}}_{t-1}$ ;
5     Set lattice  $\mathbf{G}_t^u$  and  $\gamma_t^u$  to quantize  $\tilde{\mathbf{h}}_t^u$  at rate  $R$ ;
6     Randomize dither  $\mathbf{d}_t^u$  with local seed  $\xi_t^u$ ;
7     Send  $\mathbf{G}_t^u$  and  $Q_{\mathcal{L}_{\gamma_t^u}(\mathbf{G}_t^u)}(\tilde{\mathbf{h}}_t^u + \mathbf{d}_t^u)$ ;
    Server side:
8     Compute  $Q_{\mathcal{L}_{\gamma_t^u}(\mathbf{G}_t^u)}^{\text{SDQ}}(\tilde{\mathbf{h}}_t^u)$  via  $\xi_t^u, \mathbf{d}_t^u$ ;
9   Aggregate model updates using (11) to form  $\tilde{\mathbf{w}}_t$ .
10 return  $\tilde{\mathbf{w}}_t$ 

```

This routine allows each client to adapt its lattice across FL rounds, enabling the quantizer to better match the current local update. Notably, due to the compact representation of the lattice via its generator matrix, the communication overhead associated with conveying the quantization metadata remains minimal.

B. Theoretical Analysis

The adaptive scheme in Algorithm 1, is next analytically analyzed, revealing improved convergence behavior in heterogeneous FL environments relative to its fixed, static counterpart.

1) *Updates Distortion:* Recall that the local updates transmitted from the users to the server in Algorithm 1 are compressed via lattice-based SDQ, where each edge device u is associated with a different time-varying lattice generating matrix, \mathbf{G}_t^u . This quantization inherently induces some distortion, being introduced in the FL training process. More formally, our goal is thus to quantify the difference between the ‘vanilla’-version \mathbf{w}_{t+1} in (3) to its dynamically-compressed alternative $\tilde{\mathbf{w}}_{t+1}$ in (11).

We next show that, under common assumptions used in FL analysis, the effect of the excessive distortion induced by incorporating adaptive lattice quantizers can be mitigated while recovering the desired \mathbf{w}_{t+1} as $\tilde{\mathbf{w}}_{t+1}$. Thus, the accuracy of the global learned model can be maintained. For ease of tractability, we focus on a the simple form of local-SGD (2) with FedAvg, from which convergence guarantees of other forms of local updates (e.g., mini-batch local-SGD, multiple local iterations) are known to follow [43]. Accordingly, the model updates in the following analysis are the stochastic gradients, namely,

$$\tilde{\mathbf{h}}_t^u = -\eta_t \nabla F_u(\tilde{\mathbf{w}}_t, i_t^u).$$

To begin, we adopt the following assumptions on the local datasets and on the stochastic gradient vector $\nabla F_u(\cdot, i_t^u)$:

AS1 Each dataset \mathcal{D}_u is comprised of i.i.d samples. However, different datasets can be statistically heterogeneous, i.e., arise from different distributions.

AS2 The variance of stochastic gradients is bounded:

$$\mathbb{E} \left[\|\nabla F_u(\cdot, i_t^u) - \nabla F_u(\cdot)\|^2 \right] \leq \sigma_u^2, \quad u = 1, \dots, U.$$

AS3 The quantizer employed by each user is not overloaded, for each user u and round t .

The statistical heterogeneity in AS1 is a common characteristic of FL [5], [49]. It implies that the loss surfaces can differ between users, hence the dependence on u in AS2, which is often employed in distributed learning studies [19], [43], [46], [50].

We can now bound the distance between the recovered (dynamically-quantized and stochastic) update of (11) and the desired ‘full’ non-compressed and non-stochastic one $\frac{1}{U} \sum_{u=1}^U \nabla F_u(\tilde{\mathbf{w}}_t)$, as stated in the following theorem:

Theorem III.1 (Distortion bound). *When AS1-AS3 hold, the expected distortion induced by local-SGD with lattice SDQ obeys*

$$\mathbb{E} \left[\left\| \frac{1}{U} \sum_{u=1}^U Q_{\mathcal{L}_{\gamma_t^u}(\mathbf{G}_t^u)}^{\text{SDQ}}(\nabla F_u(\tilde{\mathbf{w}}_t, i_t^u)) - \frac{1}{U} \sum_{u=1}^U \nabla F_u(\tilde{\mathbf{w}}_t) \right\|^2 \right] \leq \frac{1}{U^2} \sum_{u=1}^U (\sigma_u^2 + \sigma_{\text{SDQ}}^2(\mathcal{L}_{\gamma_t^u}(\mathbf{G}_t^u))), \quad (12)$$

where $\sigma_{\text{SDQ}}^2(\cdot)$ is given in (10).

Proof: The proof is given in Appendix B. ■

Theorem III.1 implicitly suggests that the recovered model can be made arbitrarily close to the desired one by increasing the number of edge users participating in the FL training procedure. This is because we get that (12) decreases as $1/U^2$. Besides, when the step-size η_t gradually decreases, which is known to contribute to the convergence of FL [43], [46], it follows from Theorem III.1 that the distortion decreases accordingly, further revealing its effect as the FL iterations progress, discussed next.

2) *Federated Learning Convergence:* To study the convergence of FedAvg with adaptive lattice quantizers, we further introduce the following assumption, inspired by FL convergence studies in, e.g., [19], [32], [34], [43], [46], [51]:

AS4 The local objective functions $\{F_u(\cdot)\}_{u=1}^U$ are all L -smooth and μ -strongly convex, i.e., for all $\mathbf{w}_1, \mathbf{w}_2 \in \mathbb{R}^m$

$$\begin{aligned} (\mathbf{w}_1 - \mathbf{w}_2)^T \nabla F_u(\mathbf{w}_2) + \frac{1}{2} \rho_c \|\mathbf{w}_1 - \mathbf{w}_2\|^2 &\leq F_u(\mathbf{w}_1) - F_u(\mathbf{w}_2) \leq \\ &(\mathbf{w}_1 - \mathbf{w}_2)^T \nabla F_u(\mathbf{w}_2) + \frac{1}{2} \rho_s \|\mathbf{w}_1 - \mathbf{w}_2\|^2. \end{aligned}$$

Assumption AS4 holds for a range of objective functions used in FL, including ℓ_2 -norm regularized linear regression and logistic regression [19]. To proceed, following AS1 and as in [19], [32], [34], [43], we define the heterogeneity gap,

$$\Gamma \triangleq F(\mathbf{w}_{\text{opt}}) - \sum_{u=1}^U \alpha_u \min_{\mathbf{w}} F_u(\mathbf{w}), \quad (13)$$

where \mathbf{w}_{opt} is defined in (1). Note that (13) captures the degree of heterogeneity: if $\{\mathcal{D}_u\}$ originate from the same distribution, Γ tends to zero as the training size grows, and is positive otherwise.

The following theorem characterizes the convergence of FL with local SGD training using adaptive lattice quantizers:

Theorem III.2 (FL convergence bound). *Let Assumptions AS1-AS4 hold and define $\kappa = \frac{L}{\mu}$, $\nu = \max\{8\kappa, 1\}$, and the learning rate $\eta_t = 2/(\mu(\nu + t))$. Then, for FL with users transmitting*

compressed gradients, that are quantized via lattice-based SDQ with a unique generating matrix per client, it holds that

$$\begin{aligned} & \mathbb{E}[F(\tilde{\mathbf{w}}_T)] - F(\mathbf{w}_{\text{opt}}) \\ & \leq \frac{\kappa}{\nu+T-1} \left(\frac{2}{\mu} \max_{t=1,\dots,T} B_t + \frac{\mu\nu}{2} \mathbb{E}[\|\tilde{\mathbf{w}}_1 - \mathbf{w}_{\text{opt}}\|^2] \right), \end{aligned} \quad (14)$$

where \mathbf{w}_{opt} is defined in (1), and

$$B_t := \frac{1}{U^2} \sum_{u=1}^U (\sigma_u^2 + \sigma_{\text{SDQ}}^2(\mathcal{L}_{\gamma_t}(\mathbf{G}_u^t))) + 2L\Gamma. \quad (15)$$

with Γ and $\sigma_{\text{SDQ}}^2(\cdot)$ defined in (13) and (10), respectively.

Proof: The proof is given in Appendix C. ■

Theorem III.2 rigorously bounds the difference in the objective value of the model learned via local SGD-based FL with adaptive lattice quantizers and the optimal model \mathbf{w}_{opt} , for any finite iteration index T . As such, it also frames the asymptotic convergence profile, i.e., the behavior of the bound in (14) for arbitrarily large T . Specifically, Theorem III.2 reveals that, when the sequence $\{B_t\}$ is bounded (and thus the distortion term is bounded), a convergence at a rate of $\mathcal{O}(1/T)$ is achieved. This asymptotic rate implies that as the number of iterations T progresses, the learned model converges to \mathbf{w}_{opt} with a difference decaying at the same order of convergence as FL with no compression constraints [43], [46]. Theorem III.2 thus indicates that adaptive lattice quantizers allows to incorporate compression considerations into non-i.i.d FL to be done in a manner which does not increase the order of the asymptotic convergence profile.

Theorem III.2 can be viewed as a generalization of [19, Thm. 3], which characterizes the convergence profile of SDQ-based FL with a single fixed generating matrix for all the users. This generator matrix can either be arbitrary as in [19], or optimized via [1] or [39]. Therefore, if lattice-based compressed FL can be shown to converge using a single fixed matrix across users and rounds, it raises the question of whether adaptively learning it is beneficial. This question is addressed next.

3) *Convergence Bound Minimization:* While the convergence rate is of asymptotic order $\mathcal{O}(1/T)$, the need to compress the model updates affects the convergence of the model in the non-asymptotic regime. This is revealed in Theorem III.2 via the coefficient B_t in (14). This coefficient includes several additive terms, with each stemming from a different consideration affecting the learning profile. For instance, the term depending on Γ indicates that statistical heterogeneity makes convergence slower, as noted in [43]. This heterogeneity is further captured in (15) via the averaged SDQ MSE distortion, i.e., $\sum_{u=1}^U \sigma_{\text{SDQ}}^2(\mathcal{L}_{\gamma_t}(\mathbf{G}_u^t))$. In this context, convergence is influenced by all lattices up to time step T , with the set incurring the highest error having the dominant effect. Consequently, adaptive lattices are beneficial if by adopting non-identical lattices we result with a lower convergence bound compared to the one that is obtained with identical lattices. Formally, we wish to show that $\forall t, u$ for every fixed \mathbf{G} , there exists a sequence of lattices $\{\mathbf{G}_u^t\}$ such $\sigma_{\text{SDQ}}^2(\mathcal{L}_{\gamma_t}(\mathbf{G}_u^t)) \leq \sigma_{\text{SDQ}}^2(\mathcal{L}_{\gamma_t}(\mathbf{G}))$, implying that the convergence bound is minimized by allowing the lattices to vary. This is rigorously stated in the following theorem:

Theorem III.3. Consider the quantizer of Definition II.1, using a γ -radius truncated lattice with generating matrix \mathbf{G} . Now, assume that the quantizer is not overloaded, and that the quantization rate is R . Then, the generating matrix which minimizes the MSE distortion of the SDQ scheme depends on γ , i.e.,

$$\arg \min_{\mathbf{G}} \sigma_{\text{SDQ}}^2(\mathcal{L}_{\gamma}(\mathbf{G})) = \gamma^2 \cdot \arg \min_{\mathbf{A} \in \text{SL}_L(\mathbb{R})} \mathcal{F}(\mathbf{A}, R), \quad (16)$$

where $\text{SL}_L(\mathbb{R})$ is the set of real $L \times L$ matrices with $\det(\cdot) = 1$; and $\mathcal{F}(\mathbf{A}, R)$ denotes a function depending solely on \mathbf{A} and R .

Proof: The proof is given in Appendix D. ■

To better grasp the role of γ , recall that the data is assumed to be heterogeneous among the users, and so is the distribution of the induced model weights to be compressed before transmitted to the FL server. Moreover, as the model evolves over time, this distribution is also expected to vary across time steps. Therefore, γ depends on both FL users and rounds. As this work considers compressing the updates via SDQ, γ can be viewed as an adaptive dynamic range, chosen such that it guarantees zero-overloading, or equivalently a scaling coefficient applied to the model updates; assuring the validity of Theorem II.3. In contrast, the minimizer of $\mathcal{F}(\mathbf{A}, R)$ is purely relied on geometrical aspects, and can therefore be identical for all the users. In particular, its asymptotic regime minimizer, where $R \rightarrow \infty$, is studied in classical information theory literature, e.g., [35].

In a broader perspective, Theorem III.3 implies that for heterogeneous FL, it is better (in terms of model convergence) to deviate from using identical quantization rules. This deviation, though, is not reflected in, e.g., the design of the quantizer decision cells, but rather in forming the generating matrix in a user-specific per-round manner. This is captured by (16), which reflects the interplay between the two core aspects associated with the scheme of SDQ: input-distribution invariance (i.e., universality) and zero-overloading assumption (Theorem II.3). Theorem III.3 also indicates on the potential of allowing certain amount of overloading, as preventing it directly quadratically scales the associated error. This insight and its numerical consequences on the FL model performance and convergence are systemically showcased in Section IV.

C. OLALa Algorithm

The theoretical analysis reported in the previous subsection does not consider how the local lattices $\{\mathbf{G}_t^u\}$ are chosen in Step 5 of Algorithm 1. Still, its findings reveal two key considerations as to the importance of this step in the FL procedure:

- C1 The fact that in FL (and particularly in heterogeneous settings), the distribution of the local updates can vary between rounds (t) and users (u) indicates that one can enhance the learning procedure by properly altering $\{\mathbf{G}_t^u\}$ over t and u .
- C2 The theoretical analysis assumes that the lattices are not overloaded (via AS3), which allows to rigorously characterize the distortion via Theorem II.3. When allowing some level of overloading, one can potentially achieve less distorted quantization (particularly when operating with limited quantization rates) for which, as opposed to the non-overloaded case, there is no tractable characterization.

The identification of **C1** motivates us to develop a scheme to implement Step 5 of Algorithm 1 via online lattice adaptation in a manner that can be carried out independently by each user on each round. Based on **C2**, we opt a machine learning approach for optimizing the lattices while allowing some level of overloading. To describe the resulting *OLALa* algorithm, illustrated in Fig. 2, we first discuss how we cast the local lattices as the trainable parameters of a machine learning architecture, after which we explain the loss that guides their tuning and the online learning procedure.

1) *Architecture*: We leverage deep learning tools for tuning the lattice generator matrix of user u at round t , denoted \mathbf{G}_t^u . To that aim, we formulate the lattice quantizer as a *trainable machine learning model*, parameterized by θ_t^u . This formulation is comprised of DNN augmentation and an alternative representation of the quantization operation.

DNN Augmentation: Instead of treating \mathbf{G}_t^u as a trainable parameter, we follow the deep prior approach of [45], and set it to be the output of a DNN with weights θ_t^u , fixed input \mathbf{s} , and L^2 output neurons. The reshaped DNN output is scaled to have at most 2^{LR} codewords within radius γ , and the resulting matrix, denoted $\mathbf{G}_{\theta_t^u}(\mathbf{s})$, is used as the generator matrix. This augmentation exploits the abstractness of DNNs, while stabilizing and facilitating the learning procedure.

For simplicity and following [19], we fix the quantization radius to $\gamma = 1$, and replace its role with a scaling parameter, denoted ζ_t^u . The model updates are scaled by ζ_t^u to achieve a desired level of overloading (less than 1%) within γ . This necessitates conveying ζ_t^u to the server, in addition to the DNN output $\mathbf{G}_{\theta_t^u}(\mathbf{s})$ and the quantized updates.

Reformulated Lattice Quantization: The formulation of (4) limits the ability to apply gradient-based optimization due to its continuous-to-discrete nature. Common techniques in the deep learning literature for dealing with quantized features, e.g., straight-through estimation [52], are designed to facilitate backpropagation through non-differentiable mappings (e.g., obtain the gradient of the loss with respect to the quantizer input), while we are interested in optimizing parameters of the quantizer itself. For this reason, previous studies on learned quantization [53], [54], including our preliminary work [1], utilized a *differentiable approximation* of the quantizer. These approaches require careful tuning of additional hyperparameters to achieve reliable learning, which can be done in offline training (where one can explore various hyperparameters), but is not suitable for our online learning setting.

To cope with this, we introduce an *exact* reformulation of (4) which supports gradient-based learning. To that aim, for a (possibly finite) lattice with generator matrix \mathbf{G} , denoted $\mathcal{L}(\mathbf{G})$, we define the set of lattice point indices

$$\mathcal{I}_{\mathcal{L}(\mathbf{G})} \triangleq \{\mathbf{l} \in \mathbb{Z}^L : \mathbf{G}\mathbf{l} \in \mathcal{L}(\mathbf{G})\}. \quad (17)$$

Using (17), we equivalently write the lattice quantizer (4) as

$$Q_{\mathcal{L}(\mathbf{G})}(\mathbf{x}) = \mathbf{G} \arg \min_{\mathbf{l} \in \mathcal{I}_{\mathcal{L}(\mathbf{G})}} \|\mathbf{x} - \mathbf{G}\mathbf{l}\|. \quad (18)$$

The reformulation of (4) as (18) still includes the non-differentiable $\arg \min$ operator. However, it allows one to form a computation graph that enables training the parameters

dictating \mathbf{G} via gradient-based methods due to its *linear dependence* of \mathbf{G} . Specifically, using (18), one can approximate

$$\nabla_{\theta} Q_{\mathcal{L}(\mathbf{G}_{\theta}(\mathbf{s}))}(\mathbf{x}) \approx (\nabla_{\theta} \mathbf{G}_{\theta}(\mathbf{s})) \arg \min_{\mathbf{l} \in \mathcal{I}_{\mathcal{L}(\mathbf{G}_{\theta}(\mathbf{s}))}} \|\mathbf{x} - \mathbf{G}_{\theta}(\mathbf{s})\mathbf{l}\|, \quad (19)$$

in which the $\arg \min$ statement can be viewed as a form of *stop gradient* [25].

2) *Loss Function*: Since *OLALa* is designed to adapt the local lattices by casting their operation as a machine learning architecture, their tuning requires formulating a data-driven loss function. Note that the setting of the local lattices is carried out in Step 5 of Algorithm 1, i.e., after local training (Step 4). Thus, the data used for online learning by user u at round t is the current global model $\tilde{\mathbf{w}}_t$ and its local update $\tilde{\mathbf{h}}_t^u$.

Using the model and its local updates as online learning data, we formulate two candidate empirical risk objectives:

- *Empirical MSE*, i.e., minimize quantization distortion,

$$\tilde{F}_{\mathbf{w}, \mathbf{h}}^u(\theta) = \left\| \mathbf{h} - Q_{\mathcal{L}_{\gamma}(\mathbf{G}_{\theta}(\mathbf{s}))}^{\text{SDQ}}(\mathbf{h}) \right\|^2. \quad (20)$$

- *Learning Objective* using the local FL losses (as in (1))

$$\tilde{F}_{\mathbf{w}}^u(\theta) = F_u\left(\mathbf{w} + Q_{\mathcal{L}_{\gamma}(\mathbf{G}_{\theta}(\mathbf{s}))}^{\text{SDQ}}(\mathbf{h})\right). \quad (21)$$

The loss in (21) boosts a form of *task-based quantization*, as the quantizer is tuned based on the overall learning task, as opposed to the MSE loss in (20), which seeks standard distortion minimization. However, as we view the local model as our data for online learning, (20) has the gain of supporting mini-batch based optimization, as it can be computed for any set of sub-vectors of $\tilde{\mathbf{w}}_t^u$, while (21) requires the entire vector $\tilde{\mathbf{w}}_t^u$.

3) *Online Training*: The loss functions enable unsupervised online learning of the lattices, as, e.g., no ground-truth digital representation is required. The ability to compute the gradients with respect to the lattice generator matrix via (19) enables training using conventional deep learning optimizers based on first-order methods. An example using mini-batch SGD (which, when using the loss (21), is applicable with $\beta = 1$ batch per epoch) is formulated as Algorithm 2. Once training is concluded, i.e., θ_t^u is learned, the resulting $\mathbf{G}_{\theta_t^u}(\mathbf{s})$ is used for lattice SDQ in Step 5 of the overall Algorithm 1.

Algorithm 2: Online Lattice Learning at User u , Round t

Init: Randomize θ , fix learning rate η , epochs i_{\max} , input \mathbf{s} , and number of batches β
Input: Current model $\tilde{\mathbf{w}}_t$ and update $\tilde{\mathbf{h}}_t^u$
1 **for** $i = 0 \dots i_{\max} - 1$ **do**
2 Randomly divide input into L -length M sub-vectors;
3 Randomly
4 divide M -size data into batches $\{\mathbf{w}_b, \mathbf{h}_b\}_{b=1}^{\beta}$;
5 **for** $b = 0, \dots, \beta - 1$ **do**
6 Compute batch loss $\tilde{F}_{\mathbf{w}_b, \mathbf{h}_b}^u(\theta)$ via (20) or (21);
7 Update $\theta \leftarrow \theta - \eta \nabla_{\theta} \tilde{F}_{\mathbf{w}_b, \mathbf{h}_b}^u(\theta)$;
8 Set $\theta_t^u \leftarrow \theta$;
Output: Generator matrix $\mathbf{G}_{\theta_t^u}(\mathbf{s})$

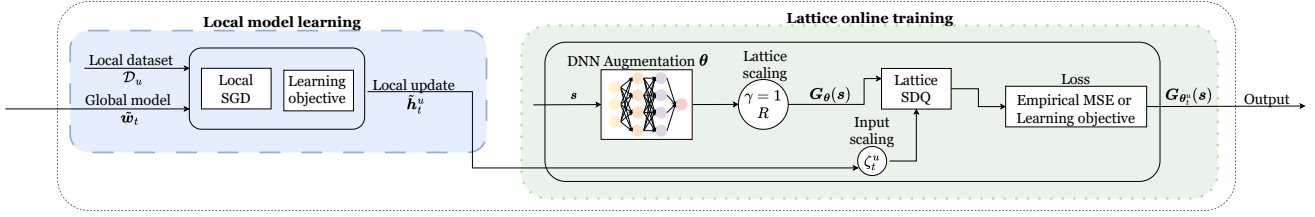


Fig. 2: Overview of OLALa at user u at time-step t , performing local model (left) and lattice (right) learning using input \tilde{w}_t to form the generator matrix $\mathbf{G}_{\theta_t^u}(s)$.

D. Discussion

The proposed OLALa framework introduces a novel mechanism for incorporating adaptive lattice quantization in FL. Our key insight is the identification of the value in tailoring the lattice quantizer to the local update at each user and communication round, thereby enabling more accurate and efficient model update transmission. OLALa enables such adaptation by allowing each user to learn and apply a custom lattice, represented compactly through its $L \times L$ generator matrix. This compact representation is independent of the quantization rate (as opposed to generic vector quantizers, whose representation requires sharing a complete rate-specific codebook), rendering the communication overhead of transmitting the quantizer metadata negligible, particularly in the context of training large-scale DNNs. Beyond its practical advantages, the use of structured lattice codes also introduces theoretical tractability into the analysis of the resulting quantization error and its propagation through the FL training process.

From a computational standpoint, the added complexity introduced by OLALa over fixed-lattice FL stems primarily from the need to learn the generator matrix during local training. This involves evaluating a compact neural network and computing its gradients on limited data (the model weights), which is modest in scale compared to the training of deep models on large data sets, as already done locally in FL. As such, the overhead is minimal when assessed over typical FL training routines, where the majority of computational effort remains focused on optimizing the global model parameters. Furthermore, our implementation ensures that the generator matrix can be efficiently updated using standard optimization routines with minor additional latency.

OLALa offers multiple modes of operation depending on the learning objective and desired granularity of adaptation. We investigate two training losses for learning the lattice: a learning-oriented loss that encourages FL performance, and a distortion-oriented MSE loss that directly minimizes quantization error. Our empirical results indicate that both losses are effective, with the MSE loss often yielding better quantizers in terms of reconstruction error, at the cost of increased sensitivity to optimization instability. Flexibility is also provided in the spatial and temporal granularity of lattice learning. OLALa supports per-user-per-round adaptation, but can also be restricted to learning a fixed lattice per user or even a globally shared lattice across all users, potentially via offline training. Nonetheless, our results consistently show that the dynamic, online adaptation offered by OLALa leads to significantly improved performance over these static alternatives, justifying the added training complexity.

Several potential extensions of OLALa are left for future work.

In our implementation, the number of codewords in the lattice is controlled via a scaling radius γ , but one may consider alternative mechanisms to enforce a fixed codebook size, such as entropy-constrained quantization [55] or volume-preserving projections. Additionally, we learn the generator matrix indirectly via a compact neural network with a fixed input to ensure numerical stability and regularization. Future studies may explore direct optimization of the generator matrix, adopt alternative parameterizations that improve convergence or expressivity, and even consider designing machine learning models to map the weights into the lattice generator matrix. Finally, OLALa currently assumes a fixed distribution for the subtractive dither; extending the framework to learn or adapt the dither distribution in conjunction with the lattice may further enhance performance and robustness.

IV. EXPERIMENTAL STUDY

We next numerically assess heterogeneous FL with adaptive lattice learning via OLALa¹. We first detail the experimental setup in Subsection IV-A; after which we evaluate the performance of the learned lattices in Subsection IV-B, as well as that of the FL global model trained using them in Subsection IV-C.

A. Experimental Setup

1) *Learning Tasks and Data Partitioning*: To evaluate the performance of OLALa, we consider two canonical FL tasks with distinct data sets and architectures: handwritten digit classification using MNIST and natural image classification using CIFAR-10.

MNIST Classification: The first task involves federated training over the MNIST dataset, which consists of 28×28 grayscale images of handwritten digits. The dataset includes 60,000 training samples and 10,000 test samples. Local training on each user is carried out using SGD with a learning rate of 0.1, and the classification loss is computed using the standard cross-entropy loss. We examine three different DNNs:

- **Linear**: A simple linear regression model.
- **MLP**: A fully-connected DNN with two hidden layers and ReLU activations.
- **CNN**: A DNN with two convolutional layers followed by two fully connected layers with ReLU activations and max-pooling.

The FL process is run for 40 global communication rounds, each comprising 100 local SGD steps. Lattice adaptation in OLALa is performed every 10 local steps.

¹The source code used in our experimental study, including all the hyper-parameters, is available online at <https://github.com/Maya-Simhi/OLALa>.

CIFAR-10 Classification: The second task uses the CIFAR-10 dataset, which comprises 32×32 RGB images categorized into 10 natural image classes, with 50,000 training and 10,000 test examples. The trained model is a CNN consisting of three convolutional layers, followed by four fully connected layers, with ReLU activations, max-pooling, and dropout layers. Local training employs SGD with a learning rate of 0.003, using cross-entropy loss. The system is run for 100 global communication rounds, each containing 1500 local iterations. Lattice learning in OLALa is updated every 100 local steps.

To emulate user heterogeneity, both tasks employ a non-i.i.d. data partitioning across $U = 5$ users. Each user is assigned samples from three classes, with a one-class overlap between consecutive users. Specifically, user u (indexed from 0 to 4) is assigned classes $\{2u, 2u + 1, 2u + 2\}$, modulo 10. This partitioning ensures both sufficient local variation and partial class overlap, achieving heterogeneous FL while ensuring that each user’s local learning impacts the global model. The setup is particularly useful for evaluating the effectiveness and fairness of user-specific quantization, such that no individual client becomes disproportionately detrimental to the training performance due to mismatched quantization.

2) *Benchmarks:* To evaluate the effectiveness of OLALa, we compare it against several FL baselines that represent different strategies for lattice quantization. For all lattice quantizers, we use dimension $d = 2$, and apply the same scaling scheme as in OLALa, i.e., we scale the generator matrix to achieve the quantization rate (which differs between tests) within a unit radius, and scale the input to meet overloading probability of up to 0.5%.

Non-Compressed FL: As an upper-bound benchmark, we consider an FL setup with no quantization. This represents the best achievable performance in terms of accuracy, but with maximal communication overhead.

Fixed Lattice Quantization: This baseline uses predefined lattice quantizers that remain fixed across all users and throughout the entire training process. We consider three generator matrices taken from the lattice quantization literature [56]:

- Hexagonal lattice $\mathbf{G}_{\text{Hex}} = \begin{bmatrix} 1 & \frac{1}{2} \\ 0 & \frac{\sqrt{3}}{2} \end{bmatrix}$.
- D_2 lattice $\mathbf{G}_{D_2} = \begin{bmatrix} 2 & 0 \\ 1 & -1 \end{bmatrix}$.
- A_2 lattice $\mathbf{G}_{A_2} = \begin{bmatrix} \sqrt{2} & 0 \\ -0.7071 & 1.2247 \end{bmatrix}$.

Learned Static Lattices: This baseline includes two variants of OLALa in which the lattice generator matrix is learned once using data-driven optimization, but remains fixed throughout the FL process. We consider two types of learned static lattices:

- *Global static*, where a single lattice is learned offline and used by all users.
- *User-dependent static*, where each user is assigned a fixed but individually learned lattice based on its local data.

These benchmarks allow evaluating the individual gains in adaptivity across users and rounds of OLALa.

B. Adaptive Lattice Learning Evaluation

Lattice Adaptation: We begin our empirical study by investigating the internal behavior of OLALa, focusing on its

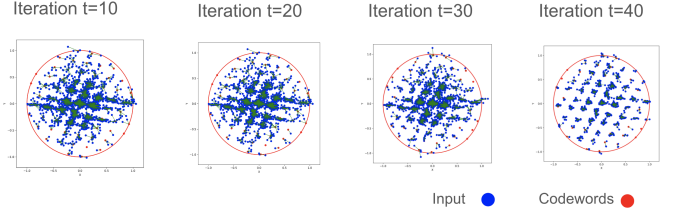


Fig. 3: Evolution of OLALa’s lattice quantizer over training rounds for User 1 on MNIST. Blue dots represent scaled weights, red dots denote codewords, red circle is the support radius γ , and green lines connect each weight to its nearest codeword.

ability to learn the quantization lattice in an online manner. To that aim, we first assess how OLALa adapts the lattice generator matrix over time, by visualizing the learned quantizer of a representative user during training on MNIST. We use a quantization rate of $R = 3$ (64 codewords at $d = 2$) and plot the lattice configuration every 10 global communication rounds. As shown in Fig. 3, each plot depicts the scaled local model weights (blue), the quantizer codewords (red), the support radius γ (red circle), and the connection between each weight and its nearest codeword (green lines).

The results clearly illustrate that the generator matrix evolves throughout the learning process. Early in training, the codewords are not well aligned with the distribution of the model weights, leading to visible mismatches (green lines). As training progresses, the quantizer becomes increasingly aligned with the model weights: the codewords spread more effectively across the input space, and the number and length of the green lines decrease. These observations support the conclusion that our online adaptation enables accurate and refined quantization.

Adaptation Loss: We next evaluate how the choice of loss function used to guide lattice adaptation affects performance. Specifically, we compare three candidate loss measures: the learned objective (accuracy) as in (21); the MSE as in (20); and a similar distortion-oriented loss, given by the (negative) signal-to-noise ratio (SNR), defined as

$$-\text{SNR} = -\|\mathbf{h}\|^2 / \left\| \mathbf{h} - Q_{\mathcal{L}_\gamma(\mathbf{G}_\theta(s))}^{\text{SDQ}}(\mathbf{h}) \right\|^2.$$

While the accuracy-based loss is task-oriented, SNR and MSE directly target the distortion induced by quantization.

Table I reports the resulting performance for different learning rates when training a CNN model on MNIST at $R = 3$. All three loss functions yield useful gradients for optimizing the lattice, but their behaviors differ significantly. The objective-based loss leads to relatively stable performance across a broad range of learning rates, indicating robustness to hyperparameter settings. In contrast, distortion-oriented objectives (SNR and MSE) can achieve higher performance when properly tuned, but exhibit greater sensitivity to the learning rate. These findings suggest that while distortion-based objectives may offer improved quantization quality, care must be taken when selecting the learning rate to avoid instability. Accuracy-based objectives, though less aggressive in minimizing distortion, provide a stable and reliable alternative.

Quantization Overloading: We proceed to investigate the impact of allowing a controlled degree of overloading on the final learning accuracy. While traditional lattice quantization

Learning Rate	Accuracy	SNR	MSE
1e-9	81.43%	71.60%	76.94%
1e-8	81.43%	82.85%	84.01%
1e-7	81.86%	89.61%	84.51%
1e-6	81.43%	87.35%	87.08%
1e-5	81.43%	85.21%	87.12%
1e-4	81.43%	90.07%	84.67%
1e-3	81.43%	84.98%	76.72%

TABLE I: Accuracy after 40 rounds with OLALa trained with different loss functions, MNIST (CNN model, $R = 3$).

Method	-1	0%	0.5%	1%	10%	50%
OLALa	93.01%	87.05%	92.06%	90.38%	86.28%	65.70%
Static-Each	92.78%	86.80%	91.95%	90.49%	87.71%	68.17%
Static-Global	91.59%	87.78%	90.91%	91.73%	90.06%	69.22%
Fixed-Hexagon	90.36%	86.53%	88.78%	91.43%	92.89%	71.65%

TABLE II: Final test accuracy of different quantization methods on MNIST (CNN, $R = 3$) under varying overloading thresholds. “-1” denotes a heuristic allowing at most 0.05% overloading with minimum variance filtering.

designs aim to entirely avoid overloading to ensure bounded distortion, recent insights suggest that relaxing this constraint may provide performance benefits. To explore this trade-off, we evaluated the classification accuracy of the CNN model trained on MNIST using OLALa and the various baseline quantization schemes, while varying the allowable overloading level. Each setting constrains the percentage of local model weights that are permitted to fall outside the quantizer support radius γ . In addition to fixed percentage-based thresholds (ranging from 0% to 50%). We include a hybrid heuristic denoted by “-1”, which limits overloading to at most 0.3% of the update sub-vectors not deviating from their empirical mean by more than $3\times$ their empirical standard deviation.

The results, summarized in Table II, reveal several important insights. First, strictly avoiding overloading (0%) leads to noticeably degraded performance across all methods, due to excessive clipping or over-conservative scaling. Conversely, permitting large amounts of overloading (e.g., 10% – 50%) harms performance due to unbounded distortion. Moderate overloading levels (around 0.5% – 1%) strike a better balance, but the best overall performance is typically achieved with the heuristic “-1” approach, which combines principled statistical filtering with a tight bound on overload count. These results validate the design choice in OLALa to allow small, controlled overloading during quantizer adaptation.

C. Federated Learning Results

We now evaluate the effectiveness of OLALa in full federated training, comparing its performance to that of alternative quantization schemes. Two key studies are reported: the first quantifies the final learning performance achieved with varying quantization rates; the second analyzes the training dynamics over time across different learning models and datasets.

Performance vs. Quantization Rate: In this study, we assess how the quantization rate used in the lattice quantizer affects the performance of the global model. We report both the classification accuracy (averaged over the last five global rounds) and the

Rate R	2	2.5	3	3.5
Non-comp.	95.24			
OLALa	81.76 / 14.56	90.42 / 21.86	93.00 / 17.63	94.61 / 20.85
Static-Each	80.41 / 12.23	87.51 / 14.53	92.78 / 16.33	94.40 / 18.54
Static-Global	79.74 / 24.39	85.31 / 22.49	91.59 / 22.35	94.22 / 24.46
Fixed-Hexagon	57.71 / 26.61	84.63 / 20.69	90.36 / 22.16	93.29 / 24.92
Fixed-A2	74.25 / 20.29	85.96 / 21.09	90.78 / 22.78	93.43 / 24.29
Fixed-D2	77.97 / 19.00	87.26 / 16.77	90.19 / 22.79	92.89 / 21.38

TABLE III: Final accuracy (in %) / SNR for different quantization schemes on MNIST (CNN) with varying codeword counts. Accuracy is averaged over the final 5 rounds.

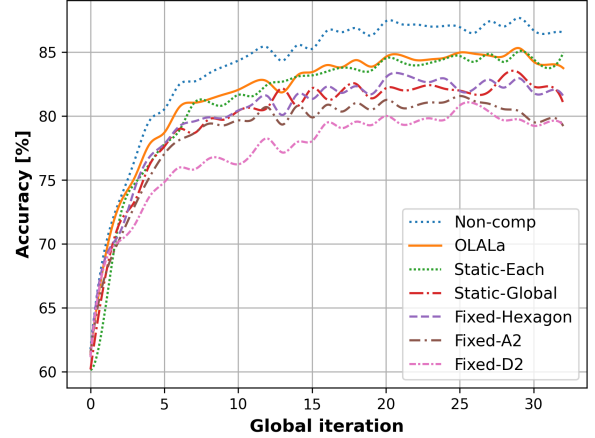


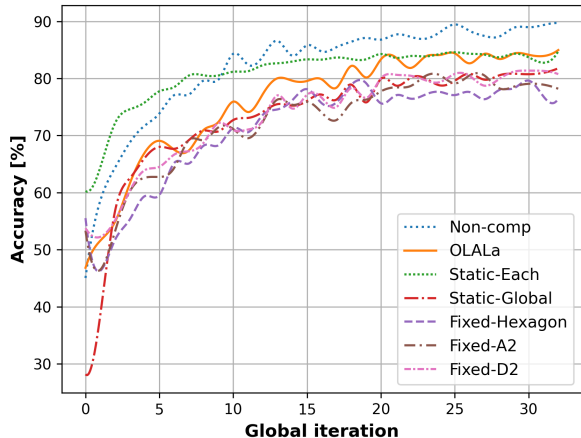
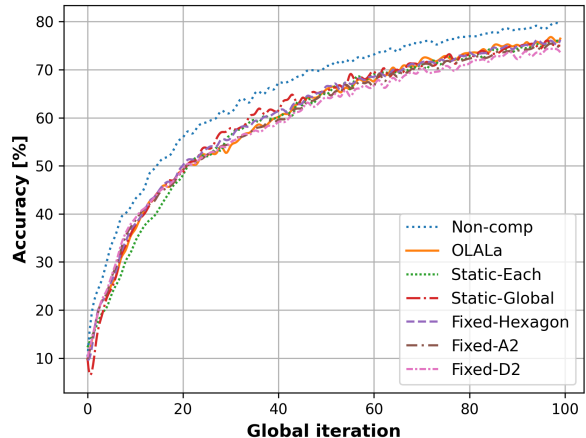
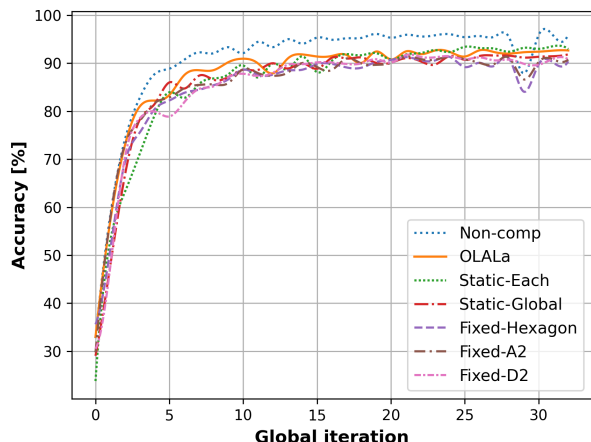
Fig. 4: Accuracy vs. training rounds, MNIST, linear model, $R = 3.5$.

SNR of the quantized model updates. The results are presented in Table III for the MNIST dataset using the CNN architecture.

Several trends emerge from Table III. First, all quantized methods show improved performance as the number of codewords increases, approaching the baseline performance of the uncompressed model (95.24%). Second, learning non-identical lattices, whether performed once per user (“Static-Each”) or adaptively during training (“OLALa”), outperforms both global and fixed lattice baselines. Notably, OLALa consistently achieves the best results across all quantization rates. Finally, we observe that a higher SNR does not always correlate with better accuracy; this discrepancy may stem from differences in how distortion is distributed across model layers and highlights the importance of task-aware quantizer optimization.

Training Dynamics: To further compare the behavior of different quantization schemes, we examine the learning curves, i.e., the evolution of validation accuracy over training rounds. We report the results three representative settings. The learning curve achieved for MNIST with the linear model and MLP (both at rate $R = 3.5$ bits per weight) are reported in Figs. 4-5, respectively, while Fig. 6 shows the corresponding learning curve achieved with the CNN model (at a slightly lower rate $R = 3$ where differences are better visible as follows from Table III). In addition, we report the learning curves achieved for CIFAR-10 with CNN in Fig. 7, where we magnify the last 30 rounds for visibility in Fig. 8. There, we considered a higher learning rate of $R = 5$ bits per weight.

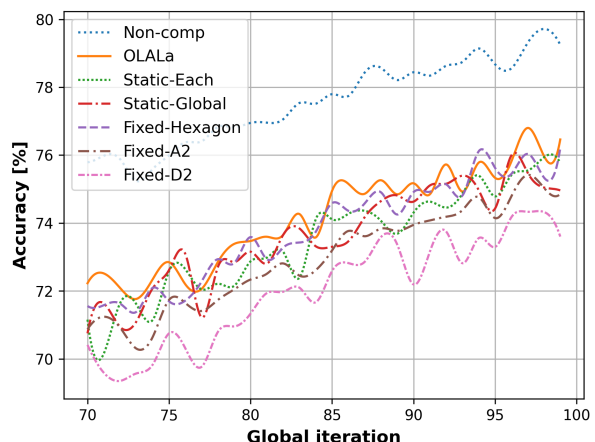
Across all configurations, we consistently observe the

Fig. 5: Accuracy vs. training rounds, MNIST, MLP, $R = 3.5$.Fig. 7: Accuracy vs. training rounds, CIFAR-10, CNN, $R = 3$ Fig. 6: Accuracy vs. training rounds, MNIST, CNN, $R = 3$.

following trends: (i) OLALa outperforms all other schemes in both convergence speed and final accuracy, especially as model complexity increases. This validates the value of round-wise adaptation to model update statistics; (ii) Using the learning framework of OLALa in a static manner can also be beneficial. Specifically, the per-user static strategy (“Static-Each”) performs closely to OLALa in early training rounds, but its lack of temporal adaptivity limits its effectiveness when update distributions change over time; (iii) Learning a single shared lattice (“Static-Global”) consistently outperforms fixed lattice baselines but lags behind personalized schemes, indicating the importance of user-specific adaptation in heterogeneous settings; (iv) Fixed lattices (e.g., Hexagon, A_2 , D_2) achieve lower performance overall and exhibit slower convergence, despite often having higher average SNRs, highlighting underscoring the need for task- and user-aware lattice learning.

V. CONCLUSIONS

We introduced an online learned adaptive lattice quantization framework for FL. Based on a theoretical analysis that highlights the potential benefits of using adaptive lattices, we

Fig. 8: Accuracy vs. training rounds, CIFAR-10, CNN, last 30 rounds, $R = 3$

proposed OLALa, which enables each client to learn and adapt a low-complexity lattice quantizer during training, allowing the quantization scheme to track the evolving distribution of local model updates. Our experimental study demonstrated that OLALa consistently outperforms fixed and statically learned lattice quantizers in terms of both convergence and final accuracy, offering a principled, efficient, and theoretically sound approach for communication-aware FL in heterogeneous environments.

APPENDIX

This appendix characterizes, under assumptions *AS1-AS4*, the distortion induced by OLALa-aided FL, as well as its convergence properties to w_{opt} for growing number of global rounds T . These results follow the proof steps of [43, Thm. 1].

It is noted that while analyzing \tilde{w}_{t+1} in (11), there are two different sources of randomness involved: a) stochastic gradients; and b) probabilistic quantization. As this pair is mutually independent with respect to both u (user index) and t (global FL iteration index); the law of total expectation can be employed in order to isolate each stochastic term. Equivalently,

each of which can be distinguished using the notation $\mathbb{E}_{\{\cdot\}}(\cdot)$. Yet, this subscript is dropped in the sequel for ease of notation.

A. Additional Notations

For convenience, we define the averaged ‘full’, stochastic, and compressed stochastic gradient, respectively, as follows:

$$\mathbf{g}_t \triangleq \frac{1}{U} \sum_{u=1}^U \nabla F_u(\tilde{\mathbf{w}}_t) \quad (\text{A.1})$$

$$\hat{\mathbf{g}}_t \triangleq \frac{1}{U} \sum_{u=1}^U \nabla F_u(\tilde{\mathbf{w}}_t, i_t^u) \quad (\text{A.2})$$

$$\hat{\mathbf{g}}_t^{\text{SDQ}} \triangleq \frac{1}{U} \sum_{u=1}^U Q_{\mathcal{L}_{\gamma_t^u}}^{\text{SDQ}}(\nabla F_u(\tilde{\mathbf{w}}_t, i_t^u)). \quad (\text{A.3})$$

According to [AS1](#), the stochastic gradient is an unbiased estimator of the ‘full’ one, i.e.,

$$\mathbb{E}[\hat{\mathbf{g}}_t] = \mathbf{g}_t. \quad (\text{A.4})$$

Additionally, by [AS3](#) and (8)-(9), we obtain

$$\mathbb{E}[\hat{\mathbf{g}}_t^{\text{SDQ}}] = \mathbb{E}[\hat{\mathbf{g}}_t] + \frac{1}{U} \sum_{u=1}^U \mathbb{E}[\mathbf{e}_{t,u}^{\text{SDQ}}] = \mathbf{g}_t. \quad (\text{A.5})$$

B. Proof of Theorem III.1

Using the auxiliary definitions of (A.1)-(A.3); and Theorem II.3 given [AS3](#), it holds that

$$\begin{aligned} & \mathbb{E} \left[\left\| \hat{\mathbf{g}}_t^{\text{SDQ}} - \hat{\mathbf{g}}_t + \hat{\mathbf{g}}_t - \mathbf{g}_t \right\|^2 \right] \\ &= \mathbb{E} \left[\left\| \hat{\mathbf{g}}_t^{\text{SDQ}} - \hat{\mathbf{g}}_t \right\|^2 \right] + \mathbb{E} \left[\left\| \hat{\mathbf{g}}_t - \mathbf{g}_t \right\|^2 \right] \\ &= \frac{1}{U^2} \sum_{u=1}^U \mathbb{E} \left[\left\| \mathbf{e}_{t,u}^{\text{SDQ}} \right\|^2 + \left\| \nabla F_u(\tilde{\mathbf{w}}_t, i_t^u) - \nabla F_u(\tilde{\mathbf{w}}_t) \right\|^2 \right] \\ &\stackrel{(\text{AS2})}{\leq} \frac{1}{U^2} \sum_{u=1}^U (\sigma_{\text{SDQ}}^2(\mathcal{L}_{\gamma_t^u}(\mathbf{G}_u^t)) + \sigma_u^2). \end{aligned}$$

C. Proof of Theorem III.2

We begin by stating the following lemma, and deferred its proof to Section E.

Lemma C.1 (Result of one-step SGD.). *Assume Assumption AS4 hold. If $\eta_t \leq \frac{1}{2L}$, then*

$$\begin{aligned} \mathbb{E} \left[\left\| \tilde{\mathbf{w}}_{t+1} - \mathbf{w}_{\text{opt}} \right\|^2 \right] &\leq (1 - \eta_t \mu) \mathbb{E} \left[\left\| \tilde{\mathbf{w}}_t - \mathbf{w}_{\text{opt}} \right\|^2 \right] \\ &\quad + \eta_t^2 \mathbb{E} \left[\left\| \mathbf{g}_t - \hat{\mathbf{g}}_t^{\text{SDQ}} \right\|^2 \right] + 2L\eta_t^2 \Gamma. \end{aligned}$$

Now, let $\Delta_t = \mathbb{E} \left[\left\| \tilde{\mathbf{w}}_t - \mathbf{w}_{\text{opt}} \right\|^2 \right]$. From Lemma C.1 and Theorem III.1, it follows that

$$\begin{aligned} \Delta_{t+1} &\leq (1 - \eta_t \mu) \Delta_t + \eta_t^2 B_t, \\ B_t &= \frac{1}{U^2} \sum_{u=1}^U (\sigma_u^2 + \sigma_{\text{SDQ}}^2(\mathcal{L}_{\gamma_t^u}(\mathbf{G}_u^t))) + 2L\Gamma. \end{aligned}$$

For a diminishing step-size, we set $\eta_t = \frac{\beta}{t+\nu}$ for some $\beta > \frac{1}{\mu}$ and $\nu > 0$ such that $\eta_1 \leq \frac{1}{2L}$. Then, in [\[43, Thm. 1\]](#), it is proved by induction that

$$\Delta_t \leq \frac{v_t}{\nu + t}, \quad v_t = \max \left\{ \frac{\beta^2}{\beta\mu - 1} \max_{t'=1, \dots, t} B_{t'}, (\nu + 1) \Delta_1 \right\}.$$

Following [AS4](#), $F(\cdot)$ is L -smoothness, and therefore

$$E[F(\tilde{\mathbf{w}}_t)] - F(\mathbf{w}_{\text{opt}}) \leq \frac{L}{2} \Delta_t \leq \frac{L}{2} \frac{v_t}{\nu + t}.$$

Specifically, if we choose $\beta = 2/\mu$, $\nu + 1 = \max \{8L/\mu, 1\}$, and denote $\kappa = L/\mu$, then $\eta_t = 2/(\mu(\nu + t))$. Finally, we have

$$\begin{aligned} v_t &= \max \left\{ \frac{\beta^2}{\beta\mu - 1} \max_{t'=1, \dots, t} B_{t'}, (\nu + 1) \Delta_1 \right\} \\ &\leq \frac{\beta^2}{\beta\mu - 1} \max_{t'=1, \dots, t} B_{t'} + (\nu + 1) \Delta_1 \\ &\leq \frac{4}{\mu^2} \max_{t'=1, \dots, t} B_{t'} + (\nu + 1) \Delta_1; \end{aligned}$$

and consequently,

$$\begin{aligned} E[F(\tilde{\mathbf{w}}_t)] - F(\mathbf{w}_{\text{opt}}) &\leq \frac{L}{2} \frac{v_t}{\nu + t} \\ &\leq \frac{\kappa}{\nu + t} \left(\frac{2}{\mu} \max_{t'=1, \dots, t} B_{t'} + \frac{\mu(\nu + 1)}{2} \Delta_1 \right), \end{aligned}$$

concluding the proof.

D. Proof of Theorem III.3

To prove Theorem III.3, we begin by expressing the distortion associated with SDQ using the following identity [\[35, Eq. 6-7\]](#):

$$\sigma_{\text{SDQ}}^2(\mathcal{L}_{\gamma}(\mathbf{G})) = \mathcal{G}(\mathbf{G}) \cdot \det(\mathbf{G})^{2/L}; \quad \mathcal{G}(\mathbf{G}) \triangleq \frac{1}{L} \cdot \frac{\int_{\mathcal{P}_0} \|\mathbf{x}\|^2 d\mathbf{x}}{\det(\mathbf{G})^{1+2/L}},$$

where \mathcal{P}_0 is the basic lattice cell (see Section II-B), and $\mathcal{G}(\mathbf{G})$ is coined the *normalized second-order moment* of the lattice.

Now, parameterize the generator using a scale factor a and a unit-volume shape matrix $\mathbf{A} \in \mathbb{R}^{L \times L}$ ($\det(\mathbf{A}) = 1$) via $\mathbf{G} = a\mathbf{A}$. Thus, $\det(\mathbf{G}) = a^L$, and

$$\sigma_{\text{SDQ}}^2(\mathcal{L}_{\gamma}(\mathbf{G})) = \mathcal{G}(\mathbf{A}) \cdot a^2, \quad (\text{D.1})$$

where, since $\mathcal{G}(\mathbf{G})$ is invariant to scale, $\mathcal{G}(\mathbf{G}) = \mathcal{G}(\mathbf{A})$.

According to Theorem III.3, the quantization rate is fixed to R , setting the codebook size as 2^{LR} . Consequently, following the fundamental definition of a (truncated) lattice, it holds that

$$\begin{aligned} 2^{LR} &= |\mathcal{L}_{\gamma}(a\mathbf{A})| = \left| \left\{ \mathbf{z} \in a\mathbf{A}\mathbb{Z}^L : \|\mathbf{z}\| \leq \gamma \right\} \right| \\ &\stackrel{z=a\mathbf{A}\mathbf{z}'}{=} \left| \left\{ \mathbf{z}' \in \mathbb{Z}^L : \|\mathbf{A}\mathbf{z}'\| \leq \frac{\gamma}{a} \right\} \right|. \end{aligned} \quad (\text{D.2})$$

Next, define $r_{\mathbf{A}}(R)$ as the *minimal* radius for which the count in (D.2) equals 2^{LR} , i.e.,

$$r_{\mathbf{A}}(R) = \arg \min_{r \in \mathbb{R}^+} \left\{ \left| \left\{ \mathbf{z}' \in \mathbb{Z}^L : \|\mathbf{A}\mathbf{z}'\| \leq r \right\} \right| = 2^{LR} \right\}, \quad (\text{D.3})$$

As a result, from (D.2)-(D.4), it follows that the most restricted configuration for a , in the presence of a fixed R and \mathbf{A} , is

$a = \gamma/r_{\mathbf{A}}(R)$. Then, substituting it back into the distortion term in (D.1), yields:

$$\sigma_{\text{SDQ}}^2(\mathcal{L}_\gamma(\mathbf{G})) = \mathcal{G}(\mathbf{A}) \cdot \left(\frac{\gamma}{r_{\mathbf{A}}(R)} \right)^2. \quad (\text{D.4})$$

Using (D.4), we can define the following optimization problem:

$$\arg \min_{\mathbf{G}} \sigma_{\text{SDQ}}^2(\mathcal{L}_\gamma(\mathbf{G})) = \gamma^2 \cdot \arg \min_{\mathbf{A} \in \text{SL}_L(\mathbb{R})} \frac{\mathcal{G}(\mathbf{A})}{(r_{\mathbf{A}}(R))^2}, \quad (\text{D.5})$$

where $\text{SL}_L(\mathbb{R})$ is the set of real $L \times L$ matrices with $\det(\cdot) = 1$; concluding the proof.

E. Deferred Proof of Lemma C.1

Using (11) and the auxiliary definitions of (A.1),(A.3); we have

$$\begin{aligned} & \mathbb{E} [\|\tilde{\mathbf{w}}_{t+1} - \mathbf{w}_{\text{opt}}\|^2] \\ &= \mathbb{E} [\|\tilde{\mathbf{w}}_t - \mathbf{w}_{\text{opt}} - \eta_t \mathbf{g}_t + \eta_t \mathbf{g}_t - \eta_t \hat{\mathbf{g}}_t^{\text{SDQ}}\|^2] \\ &= \mathbb{E} [\|\tilde{\mathbf{w}}_t - \mathbf{w}_{\text{opt}} - \eta_t \mathbf{g}_t\|^2] + \eta_t^2 \mathbb{E} [\|\mathbf{g}_t - \hat{\mathbf{g}}_t^{\text{SDQ}}\|^2] \\ &\quad + 2\eta_t \mathbb{E} [\langle \tilde{\mathbf{w}}_t - \mathbf{w}_{\text{opt}} - \eta_t \mathbf{g}_t, \mathbf{g}_t - \hat{\mathbf{g}}_t^{\text{SDQ}} \rangle]. \end{aligned}$$

Note that the last term is zero according to (A.5), while the second term is bounded in Lemma III.1. As for the first summand, it is splitted into three terms:

$$\begin{aligned} A &\triangleq \|\tilde{\mathbf{w}}_t - \mathbf{w}_{\text{opt}} - \eta_t \mathbf{g}_t\|^2 \\ &= \|\tilde{\mathbf{w}}_t - \mathbf{w}_{\text{opt}}\|^2 - \underbrace{2\eta_t \langle \tilde{\mathbf{w}}_t - \mathbf{w}_{\text{opt}}, \mathbf{g}_t \rangle}_{A_1} + \underbrace{\eta_t^2 \|\mathbf{g}_t\|^2}_{A_2}. \end{aligned} \quad (\text{E.1})$$

From the L -smoothness of $F_u(\cdot)$ in AS4, and noting $F_u^* = \min_{\mathbf{w}} F_u(\mathbf{w})$, it follows that

$$\|\nabla F_u(\tilde{\mathbf{w}}_t)\|^2 \leq 2L (F_u(\tilde{\mathbf{w}}_t) - F_u^*); \quad (\text{E.2})$$

that once combined with the convexity of $\|\cdot\|^2$, implies that:

$$A_2 \leq \eta_t^2 \sum_{u=1}^U \frac{1}{U} \|\nabla F_u(\tilde{\mathbf{w}}_t)\|^2 \leq \frac{2L\eta_t^2}{U} \sum_{u=1}^U (F_u(\tilde{\mathbf{w}}_t) - F_u^*). \quad (\text{E.3})$$

Note that

$$\begin{aligned} A_1 &= -2\eta_t \langle \tilde{\mathbf{w}}_t - \mathbf{w}_{\text{opt}}, \mathbf{g}_t \rangle \\ &= -2\eta_t \left\langle \tilde{\mathbf{w}}_t - \mathbf{w}_{\text{opt}}, \sum_{u=1}^U \frac{1}{U} \nabla F_u(\tilde{\mathbf{w}}_t) \right\rangle. \end{aligned} \quad (\text{E.4})$$

By the μ -strong convexity of $F_u(\cdot)$ in AS4:

$$\begin{aligned} & -\langle \tilde{\mathbf{w}}_t - \mathbf{w}_{\text{opt}}, \nabla F_u(\tilde{\mathbf{w}}_t) \rangle \\ & \leq -(F_u(\tilde{\mathbf{w}}_t) - F_u(\mathbf{w}_{\text{opt}})) - \frac{\mu}{2} \|\tilde{\mathbf{w}}_t - \mathbf{w}_{\text{opt}}\|^2. \end{aligned}$$

Combining (E.4) and (E.3) bounds into (E.1) results with

$$\begin{aligned} A &\leq \|\tilde{\mathbf{w}}_t - \mathbf{w}_{\text{opt}}\|^2 + \frac{2L\eta_t^2}{U} \sum_{u=1}^U (F_u(\tilde{\mathbf{w}}_t) - F_u^*) \\ &\quad - 2\eta_t \sum_{u=1}^U \frac{1}{U} (F_u(\tilde{\mathbf{w}}_t) - F_u(\mathbf{w}_{\text{opt}})) + \frac{\mu}{2} \|\tilde{\mathbf{w}}_t - \mathbf{w}_{\text{opt}}\|^2 \\ &= \|\tilde{\mathbf{w}}_t - \mathbf{w}_{\text{opt}}\|^2 + \frac{2L\eta_t^2}{U} \sum_{u=1}^U (F_u(\tilde{\mathbf{w}}_t) - F_u^*) \\ &\quad - 2\eta_t \sum_{u=1}^U \frac{1}{U} (F_u(\tilde{\mathbf{w}}_t) - F_u(\mathbf{w}_{\text{opt}})) - \mu\eta_t \|\tilde{\mathbf{w}}_t - \mathbf{w}_{\text{opt}}\|^2. \end{aligned}$$

Thus,

$$\begin{aligned} A &\leq (1 - \mu\eta_t) \|\tilde{\mathbf{w}}_t - \mathbf{w}_{\text{opt}}\|^2 \\ &\quad + \underbrace{\frac{2L\eta_t^2}{U} \sum_{u=1}^U (F_u(\tilde{\mathbf{w}}_t) - F_u^*) - \frac{2\eta_t}{U} \sum_{u=1}^U (F_u(\tilde{\mathbf{w}}_t) - F_u(\mathbf{w}_{\text{opt}}))}_{\triangleq A_3}. \end{aligned} \quad (\text{E.5})$$

To bound A_3 , recall that by it holds that (1) $F(\mathbf{w}_{\text{opt}}) = \sum_{u=1}^U F_u(\mathbf{w}_{\text{opt}})/U$, and consequently

$$\begin{aligned} A_3 &\stackrel{(a)}{=} \frac{\overbrace{-2\eta_t(1-L\eta_t)}^{\triangleq \gamma_t}}{U} \sum_{u=1}^U (F_u(\tilde{\mathbf{w}}_t) - F_u^*) \\ &\quad + \frac{2\eta_t}{U} \sum_{u=1}^U (F(\mathbf{w}_{\text{opt}}) - F_u^*) \stackrel{(b)}{=} \frac{-\gamma_t}{U} \sum_{u=1}^U (F_u(\tilde{\mathbf{w}}_t) - F(\mathbf{w}_{\text{opt}})) \\ &\quad + \frac{2\eta_t - \gamma_t}{U} \sum_{u=1}^U (F(\mathbf{w}_{\text{opt}}) - F_u^*) = -\gamma_t \underbrace{(F(\tilde{\mathbf{w}}_t) - F(\mathbf{w}_{\text{opt}}))}_{\geq 0} \\ &\quad + 2L\eta_t^2 \left(F(\mathbf{w}_{\text{opt}}) - \sum_{u=1}^U \frac{1}{U} F_u^* \right) \leq 2L\eta_t^2 \Gamma. \end{aligned} \quad (\text{E.6})$$

where (a) follows by adding and subtracting the term $\frac{2\eta_t}{U} \sum_{u=1}^U F_u^*$; (b) holds similarly using the term $F(\mathbf{w}_{\text{opt}})$; and the last inequality is true since it is given that $\eta_t \leq 1/(2L)$ what implies that $\gamma_t \geq 0$. Plugging in (E.6) into (E.5), we obtain:

$$A \leq (1 - \mu\eta_t) \|\tilde{\mathbf{w}}_t - \mathbf{w}_{\text{opt}}\|^2 + 2L\eta_t^2 \Gamma,$$

and taking expectation on both sides completes the proof.

REFERENCES

- [1] N. Lang, I. Assaf, O. Bokobza, and N. Shlezinger, "Data-driven lattices for vector quantization," in *IEEE International Conference on Acoustics, Speech and Signal Processing (ICASSP)*, 2024, pp. 8080–8084.
- [2] B. McMahan, E. Moore, D. Ramage, S. Hampson, and B. A. y Arcas, "Communication-efficient learning of deep networks from decentralized data," in *Artificial Intelligence and Statistics*. PMLR, 2017, pp. 1273–1282.
- [3] S. AbdulRahman *et al.*, "A survey on federated learning: The journey from centralized to distributed on-site learning and beyond," *IEEE Internet Things J.*, vol. 8, no. 7, pp. 5476–5497, 2020.
- [4] J. Wen *et al.*, "A survey on federated learning: challenges and applications," *International Journal of Machine Learning and Cybernetics*, vol. 14, no. 2, pp. 513–535, 2023.
- [5] P. Kairouz *et al.*, "Advances and open problems in federated learning," *Foundations and trends® in machine learning*, vol. 14, no. 1–2, pp. 1–210, 2021.

- [6] T. Gafni, N. Shlezinger, K. Cohen, Y. C. Eldar, and H. V. Poor, "Federated learning: A signal processing perspective," *IEEE Signal Process. Mag.*, vol. 39, no. 3, pp. 14–41, 2022.
- [7] M. Chen, N. Shlezinger, H. V. Poor, Y. C. Eldar, and S. Cui, "Communication-efficient federated learning," *Proceedings of the National Academy of Sciences*, vol. 118, no. 17, p. e2024789118, 2021.
- [8] O. Peleg, N. Lang, S. Rini, N. Shlezinger, and K. Cohen, "PAUSE: Privacy-aware active user selection for federated learning," in *IEEE International Conference on Acoustics, Speech and Signal Processing (ICASSP)*, 2025.
- [9] P. Han, S. Wang, and K. K. Leung, "Adaptive gradient sparsification for efficient federated learning: An online learning approach," in *IEEE International Conference on Distributed Computing Systems*, 2020, pp. 300–310.
- [10] A. Aji and K. Heafield, "Sparse communication for distributed gradient descent," in *Conference on Empirical Methods in Natural Language Processing*. Association for Computational Linguistics (ACL), 2017, pp. 440–445.
- [11] D. Alistarh *et al.*, "The convergence of sparsified gradient methods," *Advances in Neural Information Processing Systems*, vol. 31, 2018.
- [12] M. M. Amiri and D. Gündüz, "Machine learning at the wireless edge: Distributed stochastic gradient descent over-the-air," *IEEE Trans. Signal Process.*, vol. 68, pp. 2155–2169, 2020.
- [13] T. Sery, N. Shlezinger, K. Cohen, and Y. C. Eldar, "Over-the-air federated learning from heterogeneous data," *IEEE Trans. Signal Process.*, vol. 69, pp. 3796–3811, 2021.
- [14] K. Yang, T. Jiang, Y. Shi, and Z. Ding, "Federated learning via over-the-air computation," *IEEE Trans. Wireless Commun.*, vol. 19, no. 3, pp. 2022–2035, 2020.
- [15] Y. Chen, L. Abrahamyan, H. Sahli, and N. Deligiannis, "Learned parameter compression for efficient and privacy-preserving federated learning," *IEEE Open Journal of the Communications Society*, vol. 5, pp. 3506–3516, 2024.
- [16] D. Alistarh, D. Grubic, J. Li, R. Tomioka, and M. Vojnovic, "QSGD: Communication-efficient SGD via gradient quantization and encoding," *Advances in Neural Information Processing Systems*, vol. 30, pp. 1709–1720, 2017.
- [17] A. Reiszadeh, A. Mokhtari, H. Hassani, A. Jadbabaie, and R. Pedarsani, "Fedpaq: A communication-efficient federated learning method with periodic averaging and quantization," in *International Conference on Artificial Intelligence and Statistics*. PMLR, 2020, pp. 2021–2031.
- [18] J. Bernstein, Y.-X. Wang, K. Azzadenesheli, and A. Anandkumar, "signSGD: Compressed optimisation for non-convex problems," in *International Conference on Machine Learning*. PMLR, 2018, pp. 560–569.
- [19] N. Shlezinger, M. Chen, Y. C. Eldar, H. V. Poor, and S. Cui, "UVeQFed: Universal vector quantization for federated learning," *IEEE Trans. Signal Process.*, vol. 69, pp. 500–514, 2020.
- [20] S. Horvóth *et al.*, "Natural compression for distributed deep learning," in *Mathematical and Scientific Machine Learning*. PMLR, 2022, pp. 129–141.
- [21] Y. Wang, Y. Xu, Q. Shi, and T.-H. Chang, "Quantized federated learning under transmission delay and outage constraints," *IEEE J. Sel. Areas Commun.*, vol. 40, no. 1, pp. 323–341, 2021.
- [22] R. M. Gray and D. L. Neuhoff, "Quantization," *IEEE Trans. Inf. Theory*, vol. 44, no. 6, pp. 2325–2383, 1998.
- [23] Y. Linde, A. Buzo, and R. Gray, "An algorithm for vector quantizer design," *IEEE Trans. Commun.*, vol. 28, no. 1, pp. 84–95, 1980.
- [24] T. Kohonen, "Learning vector quantization," *Self-organizing maps*, pp. 245–261, 2001.
- [25] A. Van Den Oord and O. Vinyals, "Neural discrete representation learning," *Advances in Neural Information Processing Systems*, vol. 30, 2017.
- [26] E. Fishel, M. Malka, S. Ginzach, and N. Shlezinger, "Remote inference over dynamic links via adaptive rate deep task-oriented vector quantization," *arXiv preprint arXiv:2501.02521*, 2025.
- [27] N. Shlezinger, Y. C. Eldar, and M. R. Rodrigues, "Hardware-limited task-based quantization," *IEEE Trans. Signal Process.*, vol. 67, no. 20, pp. 5223–5238, 2019.
- [28] Y. Polyanskiy and Y. Wu, "Lecture notes on information theory," *Lecture Notes for 6.441 (MIT), ECE563 (University of Illinois Urbana-Champaign), and STAT 664 (Yale)*, 2012–2017.
- [29] R. M. Gray and T. G. Stockham, "Dithered quantizers," *IEEE Trans. Inf. Theory*, vol. 39, no. 3, pp. 805–812, 1993.
- [30] S. P. Lipshitz, R. A. Wannamaker, and J. Vanderkooy, "Quantization and dither: A theoretical survey," *Journal of the audio engineering society*, vol. 40, no. 5, pp. 355–375, 1992.
- [31] R. Zamir and M. Feder, "On universal quantization by randomized uniform/lattice quantizers," *IEEE Trans. Inf. Theory*, vol. 38, no. 2, pp. 428–436, 1992.
- [32] N. Lang, E. Sofer, T. Shaked, and N. Shlezinger, "Joint privacy enhancement and quantization in federated learning," *IEEE Trans. Signal Process.*, vol. 71, pp. 295–310, 2023.
- [33] A. M. Shahmiri, C. W. Ling, and C. T. Li, "Communication-efficient Laplace mechanism for differential privacy via random quantization," in *IEEE International Conference on Acoustics, Speech and Signal Processing (ICASSP)*, 2024, pp. 4550–4554.
- [34] N. Lang, N. Shlezinger, R. G. D'Oliveira, and S. E. Rouayheb, "Compressed private aggregation for scalable and robust federated learning over massive networks," *IEEE Trans. Mobile Comput.*, 2025, early access.
- [35] R. Zamir and M. Feder, "On lattice quantization noise," *IEEE Trans. Inf. Theory*, vol. 42, no. 4, pp. 1152–1159, 1996.
- [36] A. Gersho, "Asymptotically optimal block quantization," *IEEE Trans. Inf. Theory*, vol. 25, no. 4, pp. 373–380, 1979.
- [37] S. Lyu, Z. Wang, C. Ling, and H. Chen, "Better lattice quantizers constructed from complex integers," *IEEE Trans. Commun.*, vol. 70, no. 12, pp. 7932–7940, 2022.
- [38] E. Agrell and B. Allen, "On the best lattice quantizers," *IEEE Trans. Inf. Theory*, vol. 69, no. 12, pp. 7650–7658, 2023.
- [39] E. Agrell and T. Eriksson, "Optimization of lattices for quantization," *IEEE Trans. Inf. Theory*, vol. 44, no. 5, pp. 1814–1828, 1998.
- [40] E. Agrell, D. Pook-Kolb, and B. Allen, "Optimization and identification of lattice quantizers," *IEEE Trans. Inf. Theory*, 2025, early access.
- [41] N. Shlezinger and T. Routtenberg, "Discriminative and generative learning for linear estimation of random signals [lecture notes]," *IEEE Signal Process. Mag.*, vol. 40, no. 6, pp. 75–82, 2023.
- [42] M. Ye, X. Fang, B. Du, P. C. Yuen, and D. Tao, "Heterogeneous federated learning: State-of-the-art and research challenges," *ACM Computing Surveys*, vol. 56, no. 3, pp. 1–44, 2023.
- [43] X. Li, K. Huang, W. Yang, S. Wang, and Z. Zhang, "On the convergence of fedavg on non-iid data," in *International conference on learning representations (ICLR)*, 2020.
- [44] N. Shlezinger, Y. C. Eldar, and S. P. Boyd, "Model-based deep learning: On the intersection of deep learning and optimization," *IEEE Access*, vol. 10, pp. 115 384–115 398, 2022.
- [45] D. Ulyanov, A. Vedaldi, and V. Lempitsky, "Deep image prior," in *IEEE Conference on Computer Vision and Pattern Recognition*, 2018, pp. 9446–9454.
- [46] S. U. Stich, "Local SGD converges fast and communicates little," in *International Conference on Learning Representations*, 2019.
- [47] R. Gray, "Vector quantization," *IEEE ASSP Mag.*, vol. 1, no. 2, pp. 4–29, 1984.
- [48] E. Agrell, T. Eriksson, A. Vardy, and K. Zeger, "Closest point search in lattices," *IEEE Trans. Inf. Theory*, vol. 48, no. 8, pp. 2201–2214, 2002.
- [49] N. Shlezinger, S. Rini, and Y. C. Eldar, "The communication-aware clustered federated learning problem," in *IEEE International Symposium on Information Theory (ISIT)*, 2020, pp. 2610–2615.
- [50] Y. Zhang, M. J. Wainwright, and J. C. Duchi, "Communication-efficient algorithms for statistical optimization," *Advances in Neural Information Processing Systems*, vol. 25, 2012.
- [51] N. Lang, A. Cohen, and N. Shlezinger, "Stragglers-aware low-latency synchronous federated learning via layer-wise model updates," *IEEE Trans. Commun.*, vol. 73, no. 5, pp. 3333–3346, 2025.
- [52] M. Huh, B. Cheung, P. Agrawal, and P. Isola, "Straightening out the straight-through estimator: Overcoming optimization challenges in vector quantized networks," in *International Conference on Machine Learning*. PMLR, 2023, pp. 14 096–14 113.
- [53] N. Shlezinger, A. Amar, B. Luijten, R. J. Van Sloun, and Y. C. Eldar, "Deep task-based analog-to-digital conversion," *IEEE Trans. Signal Process.*, vol. 70, pp. 6021–6034, 2022.
- [54] T. Vol, L. Danial, and N. Shlezinger, "Learning task-based trainable neuromorphic ADCs via power-aware distillation," *IEEE Trans. Signal Process.*, vol. 73, pp. 1246–1261, 2025.
- [55] P. A. Chou, T. Lookabaugh, and R. M. Gray, "Entropy-constrained vector quantization," *IEEE Trans. Acoust., Speech, Signal Process.*, vol. 37, no. 1, pp. 31–42, 1989.
- [56] G. Nebe and N. Sloane, "A catalogue of lattices." [Online]. Available: <https://www.math.rwth-aachen.de/homes/Gabriele.Nebe/LATTICES/>